

UC Irvine

UC Irvine Previously Published Works

Title

Key Experimental Considerations When Evaluating Functional Ionic Liquids for Combined Capture and Electrochemical Conversion of CO₂

Permalink

<https://escholarship.org/uc/item/9qm8s6c3>

Authors

Dongare, Saudagar
Coskun, Oguz Kagan
Cagli, Eda
[et al.](#)

Publication Date

2024-03-05

DOI

10.1021/acs.langmuir.3c03828

Peer reviewed

Key Experimental Considerations When Evaluating Functional Ionic Liquids for Combined Capture and Electrochemical Conversion of CO₂

Published as part of Langmuir *virtual special issue* "Highlights in Interface Science and Engineering: Reactive Separations for Carbon Capture".

Saudagar Dongare, Oguz Kagan Coskun, Eda Cagli, Jared S. Stanley, Ab Qayoom Mir, Rowan S Brower, Jesús M. Velázquez, Jenny Y. Yang, Robert L Sacci, and Burcu Gurkan*



Cite This: <https://doi.org/10.1021/acs.langmuir.3c03828>



Read Online

ACCESS |



Metrics & More

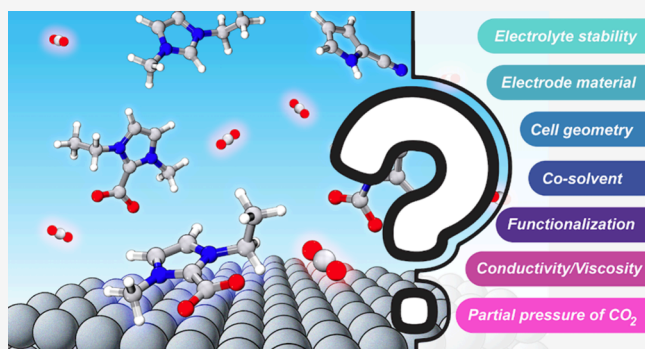


Article Recommendations



Supporting Information

ABSTRACT: Ionic liquids (ILs) are considered functional electrolytes for the electrocatalytic reduction of CO₂ (ECO₂R) due to their role in the double-layer structure formation and increased CO₂ availability at the electrode surface, which reduces the voltage requirement. However, not all ILs are the same, considering the purity and degree of the functionality of the IL. Further, there are critical experimental factors that impact the evaluation of ILs for ECO₂R including the reference electrode, working electrode construction, cosolvent selection, cell geometry, and whether the electrochemical cell is a single compartment or a divided cell. Here, we describe improved synthesis methods of imidazolium cyanopyrrolide IL for electrochemical studies in consideration of precursor composition and reaction time. We explored how IL with cosolvents (i.e. acetonitrile, dimethylformamide, dimethyl sulfoxide, propylene carbonate, and n-methyl-2-pyrrolidone) affects conductivity, CO₂ mass transport, and ECO₂R activation overpotential together with the effects of electrode materials (Sn, Ag, Au, and glassy carbon). Acetonitrile was found to be the best solvent for lowering the onset potential and increasing the catalytic current density for the production of CO owing to the enhanced ion mobility in combination with the silver electrode. Further, the ECO₂R activity of molecular catalysts Ni(cyclam)Cl₂ and iron tetraphenylsulfonato porphyrin (FeTPPS) on the carbon cloth electrode maintained high Faradaic efficiencies for CO in the presence of the IL. This study presents best practices for examining nontraditional multifunctional electrolytes amenable to integrated CO₂ capture and conversion technologies for homogeneous and heterogeneous ECO₂R.



INTRODUCTION

There are limited options for solvent/electrolyte combinations for the combined capture and electrochemical conversion of CO₂. Aqueous electrolytes^{1,2} have low CO₂ solubility and suffer from a limited electrochemical window, thus resulting in hydrogen evolution reaction (HER) competition with the electrocatalytic reduction of CO₂ (ECO₂R) reaction. Organic electrolytes² that are composed of molecular solvents and supporting salts also present limited CO₂ solubility in addition to being flammable and highly volatile. Ionic liquids (ILs)^{3,4} are the only class of solvents that are not limited by the same competing reactions or low CO₂ solubility for a combined capture and conversion process. ILs are salts that melt below 100 °C; they have very low or negligible vapor pressures and high electrochemical stability.⁵

Many non-functional ILs are commercially available,⁶ however, functionalized ILs tuned for specific applications

are often not. Even with commercial ILs, the presence of trace level of impurities (e.g., moisture, metal-ions, or halides) negatively impact electrochemical stability and other physical properties, thus making it difficult to reproduce data and accurately interpret experimental results.⁷ A simple protocol to functionalize ILs involves replacing the halide of the salt precursor with an organic or inorganic anion bearing the functional moiety.⁸ Alternatively, the functional moiety may be appended to the cation through alkylation.⁹ The former can be

Received: December 11, 2023

Revised: February 23, 2024

Accepted: February 23, 2024

achieved via direct mixing or using ion exchange methodologies. Typically, a higher purity is achieved by anion exchange via column chromatography followed by a metathesis reaction. These protocols have not been optimized for scalable functional IL synthesis with the high purity required for electrochemical studies. Here, the reaction times and stoichiometry were examined for improving the larger scale synthesis of 1-ethyl-3-methylimidazolium 2-cyanopyrrolide, [EMIM][2-CNpyr], which has been demonstrated as a superior IL in terms of CO₂ capture capacity under low partial pressures^{10,11} and ECO₂R performance for CO₂-to-CO over Ag¹² and CO₂-to-C₂₊ over Cu¹³ electrodes. According to these studies, upon CO₂ exposure, carboxylate ([EMIM]⁺-CO₂⁻) forms as the dominant product through the deprotonation of the α -carbon on [EMIM]⁺; the proton is transferred to the anion, thus forming the neutral species 2-CNpyrH. In parallel, CO₂ also binds to the anion forming carbamate ([2-CNpyr]-CO₂⁻). As such, functional ILs present unique behavior near polarized surfaces. It is imperative to perform ECO₂R with appropriate techniques and careful analysis that allow comparisons of the catalytic behavior of ILs.

One of the earliest examined ILs for ECO₂R is the commercially available imidazolium tetrafluoroborate, [EMIM][BF₄].⁴ This IL was shown to reduce the energy requirement of the formation of CO₂^{•-} anion radical, which is believed to be the first step and the rate-determining step (RDS) in the mechanism for ECO₂R. Further, this IL was shown to stabilize the reaction intermediates on the electrode surface, thus enhancing ECO₂R selectivity while suppressing competitive HER.¹⁴ Since then, imidazolium-based ILs have been examined for ECO₂R and they have demonstrated selectivity for CO production on a Ag working electrode.^{15,16} However, for practical ECO₂R studies, the viscosity of neat ILs is too high (typically >20 mPa·s at 25 °C); moreover, the viscosity of the functionalized ILs increases with CO₂ saturation, thus limiting current response and product yield. Therefore, organic solvents were utilized as diluents in IL electrolytes to enhance ECO₂R performance.¹⁷ Recent studies highlighted the significant influence of the electrolyte composition on the rates of CO₂ reduction and H₂ evolution.²

When examining the influence of the electrolyte composition, purity is an important criterion since metal-ion or halide impurities (e.g., Pb²⁺, Cl⁻, Br⁻, and I⁻) are shown to deactivate the electrode due to deposition of these impurities during electrolysis, blocking catalytic active sites and promoting HER.¹⁸ Further, water is a common impurity in IL electrolytes due to the hydrophilicity of the IL; trace amounts of water are often unavoidable even with careful sample preparation and handling.¹⁹ Recently, Guo et al.²⁰ studied the ECO₂R kinetics in [EMIM][BF₄]/acetonitrile electrolyte with varying the water content from 0.03 to 1.01 M on Ag, where the primary ECO₂R product was CO (~85% FE with 0.03 M water). However, the formations of H₂ and formate are reported at higher water contents due to the change in the interfacial microenvironment caused by water. Although not IL-based, Figueiredo et al.²¹ examined the microenvironment in a 0.1 M tetraethylammonium tetrafluoroborate ([TEA][BF₄])/acetonitrile electrolyte containing trace amounts of water on Cu by *in situ* FTIR spectroscopy. The primary ECO₂R product was CO; however, the formation of bicarbonate and carbonate was also suggested, and the amount produced was influenced by the residual water. The formation of carbonate and bicarbonate species seems to result from a solution-phase reaction of CO₂

with electrochemically generated OH⁻ from water reduction. Therefore, even a residual amount of water maybe relevant to examine in ECO₂R with nonaqueous electrolytes, including ILs.

Besides electrolyte composition and the choice of the electrode, the configuration of the electrochemical cell stands as a critical parameter impacting mass transport behavior that ultimately influences the feasibility of ECO₂R.²² Most of the fundamental science studies use electrochemical cells with stationary electrolytes, whereas practical applications or applied research use cells with flowing electrolytes. There is variability in electrode placement in static cells and varied flow conditions in flow cells. Therefore, there is inconsistency in comparing the results between the reactive systems that operate on widely varied length and time scales. Additionally, one must consider the selection of the analytical methodology for ECO₂R product quantification. For gaseous products, online methods such as gas chromatography (GC)²³ and differential electrochemical mass spectrometry (DEMS)²⁴ with their improved detection limits²⁵ are suitable. Liquid products can be quantified using high-performance liquid chromatography (HPLC)¹⁷ or (for ionic species like formate) ion-exchange chromatography,²⁶ and nuclear magnetic resonance spectroscopy (NMR),¹³ and combinations thereof. Among the quantitative online techniques, GC and NMR have been widely used due to their wide availability and ability to detect a broad range of products without any interference of the solvent, which can be problematic using DEMS.

While there has been a considerable number of reports detailing the study of heterogeneous electrocatalysis in ILs, there are fewer reports of homogeneous molecular electrocatalysis in ILs.^{27–29} The presence of an IL with a high CO₂ solubility increases the CO₂ availability in the vicinity of the molecular catalyst, which can have an impact on the rate of CO₂ reduction. These effects are underexplored within the homogeneous systems.

Here, we examined the influence of a reactive IL and the synergy between the IL and the model molecular catalysts on the homogeneous and heterogeneous electrocatalysis of CO₂ conversion reactions. More specifically, we report an improved synthetic method for the preparation of imidazolium-based CO₂-reactive ILs with a basic anion as an example for increased purity and scalability for adaption in ECO₂R. As CO₂-reactive ILs typically present high viscosities and condensed interfacial behavior near the electrode, different organic cosolvents, listed in Table 1, are examined in terms of tuning viscosity, conductivity, and CO₂ solubility. The impact of electrode material (Ag, Au, Sn, and glassy carbon) and electrochemical cell configuration on the CO₂ reduction product distribution and electrolyte stability during ECO₂R were also investigated. Further, iron tetraphenylsulfonatoporphyrin (FeTPPS) and nickel cyclam (Ni(cyclam)Cl₂ or Ni(cyclam)⁺²), representing common molecular catalysts, were studied in the presence of the IL for ECO₂R with a carbon cloth electrode. The latter catalyst has high HER activity using carbon working electrodes under aqueous conditions.^{30,31} The hypothesis being probed in this study is the elimination of HER selectivity during ECO₂R facilitated by molecular catalysts in the presence of the IL in a polar aprotic solvent to achieve quantitative Faradaic yield for CO. In addition to these investigations, electrochemical methods better suited for the characterization of small-volume IL-based electrolytes are discussed. This study aims to bring

Table 1. CO₂ Solubility and Physical Properties of Organic Solvents Used in the Study^{32–35} in Comparison to the IL, [EMIM][2-CNpyr]^{36a}

solvent	CO ₂ solubility (mmol·kg ⁻¹)	viscosity (mPa·s)	vapor pressure (Torr)	boiling point (°C)
acetonitrile	399	0.341	88.8	82
dimethylformamide (DMF)	205	0.802	2.3	153
dimethyl sulfoxide (DMSO)	119	1.99	0.417	189
N-methylpyrrolidinone (NMP)	147	1.89	0.33	202
propylene carbonate (PC)	112	2.53	0.13	242
[EMIM][2-CNpyr]	4573	67.8	N/A	N/A

^aCO₂ solubility, viscosity, and vapor pressure are measured at 25 °C.

attention to the critical considerations when examining nontraditional multifunctional electrolytes that are amenable for integrated CO₂ capture and conversion technologies for ECO₂R.

EXPERIMENTAL SECTION

Materials. The anion precursor, pyrrole 2-carbonitrile (2-CNpyrH) (99%, Alfa Aesar), was used as received. The cation precursor 1-ethyl-3-methylimidazolium bromide ([EMIM][Br]) was synthesized from 1-methylimidazole (>99%, TCI) and bromo ethane (99%, TCI), while 1-ethyl-3-methylimidazolium chloride ([EMIM][Cl], 98%, Sigma-Aldrich) was used as received and dried under vacuum at 60 °C. Hydroxide-form anion exchange resin (AER) (A600-OH, Purolite) was packed into a column and washed with methanol prior to use. A cation exchange membrane Nafion-117 was purchased from Fuel Cell Store, USA. As-received Nafion-117 was pretreated with H₂O₂ and H₂SO₄ to remove organic impurities and improve the proton conductivity, respectively. The detailed Nafion-117 pretreatment procedure is reported elsewhere.³⁷ The pretreated Nafion-117 membrane was stored in 0.1 M tetraethylammonium perchlorate/acetonitrile solution.

Other chemicals, including silver nitrate (0.171N, Ricca), methanol (99.8%, HPLC grade, Fischer), acetonitrile (99.8%, HPLC grade, Fischer), and DMSO-*d*₆ (99.9%, Thermo Scientific) were used as received. For the supporting electrolyte, as received, tetraethylammonium perchlorate (TEAP, ≥98%, BeanTown Chemical) was dried overnight at 100 °C under vacuum to remove trace volatiles. For nuclear magnetic resonance (NMR) spectroscopy (Bruker Ascend 500 MHz), dimethyl sulfoxide-*d*₆ (DMSO-*d*₆, 99.9% (Isotopic),

Thermo Scientific) was used in sample preparation. Iron tetraphenylsulfonato porphyrin (FeTPPS) was purchased from Frontier Scientific and used as received. 2,2,2-Trifluoroethanol (TFE) and tetrabutylammonium hexafluorophosphate (TBAPF₆) were purchased from TCI. TBAPF₆ was recrystallized three times from ethanol. Ni(cyclam)Cl₂ was synthesized according to the reported method.³⁰

Modified IL Synthesis Procedure. Reaction conditions were improved to facilitate the scalable IL synthesis while considering the purity through modification of the reaction time, starting material stoichiometries, and solvent use. First, the cation precursor, 1-ethyl-3-methylimidazolium bromide ([EMIM][Br]), was synthesized by solventless quaternization/Menshutkin reaction and further converted to [EMIM][2-CNpyr] following the previously reported procedure^{36,38–40} with some modifications. The major specific modification was the use of an anion exchange column for the conversion of [EMIM][Br] to [EMIM][OH]. The obtained [EMIM][OH] solution was concentrated, and then, an equimolar amount of pyrrole 2-carbonitrile was added; the synthesis solution was magnetically stirred effectively at 22 °C for 24 h under atmospheric conditions. After confirming the successful IL synthesis with minimal impurity, we then scaled up the synthesis batch to 40 g using the necessary starting materials (0.2 mmol of [EMIM][Br] and equimolar amount of pyrrole-2-carbonitrile). The detailed procedure for IL synthesis is provided in the [Supporting Information](#).

Electrochemical Methods. Linear Sweep Voltammetry (LSV).

Unless otherwise noted, all voltammetric measurements with diluted IL solutions were performed in a 5 mL single-compartment, three-electrode cell (Pine Research, USA) with a Bio-Logic VSP-300 multichannel potentiostat. A standard disk electrode (glassy carbon, Ag, and Au; purchased from BASi) with 1.6 mm diameter was used as the WE. LSVs with tin (Sn, 98.8%, Millipore Sigma) were performed with a 2 × 2 mm sheet. Prior to experiments, the disk electrodes were polished with a 0.30 μm fine alumina suspension (Pine research) and then rinsed with ultrapure water followed by sonication in ultrapure acetonitrile. A Pt wire was used as the counter electrode, and nonaqueous Ag/Ag⁺ was used as the reference electrode. The reference electrode was prepared by immersing polished Ag wire into 0.1 M TEAP/acetonitrile containing 10 mM AgNO₃ with a porous frit at one end. Potential was scanned from open circuit potential (OCP) to −2.3 or −2.5 V with a scan rate of 10 mV/s.

T-Cell Voltammetry. Considering the sensitivity of ILs toward moisture, the electrochemical window of the pure IL was measured using cyclic voltammetry (CV) in an airtight T-cell⁴¹ configuration with minimized sample size (see [Figure 1a](#)). Accordingly, the required IL volume can be as low as 20 to 200 μL, depending on the size of the reference electrode. The atmosphere can be controlled by having a flow of a dry inert gas, thus eliminating the effects of water and dissolved reactive gases. A small portion of a plastic disposable pipet tip or a heat-shrink tube fitted to the electrode diameter was securely

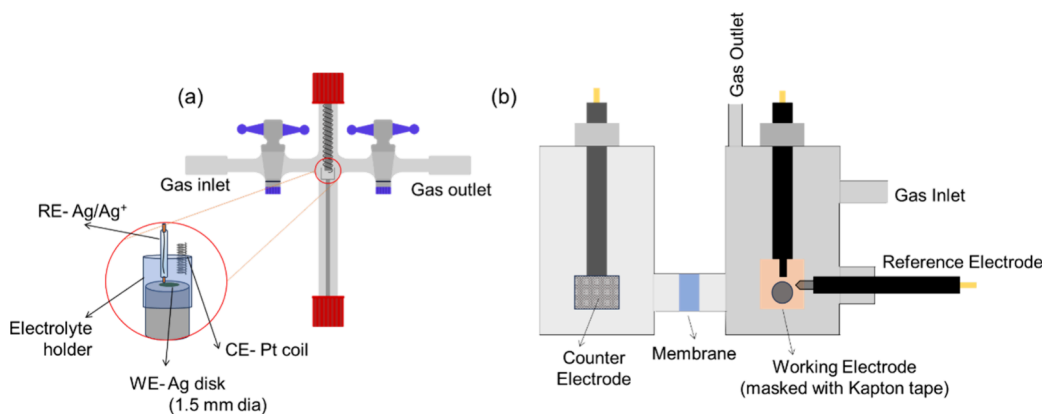


Figure 1. (a) Cross section of the low-volume T-cell employed for cyclic voltammetry and microvoltammetry measurements using a 200 μL electrolyte sample under controlled gas atmosphere conditions. (b) Schematics of the two-compartment H-cell used for bulk electrolysis experiments a minimum amount of electrolytes (5 mL) where the distance between working and counter electrodes was 5 cm.

placed around the end of the working electrode (Ag disk, 1.5 mm) to create a cavity within which 200 μL of the IL sample was placed. The reference electrode (Ag/Ag⁺) and counter electrode (Pt wire) were immersed from the top, as shown in Figure 1a. This configuration allows placement of the reference electrode close to the working electrode.

The microvoltammetry experiments with the Ag microelectrode (diameter: 12 μm (area: $1.23 \times 10^{-6} \text{ cm}^2$), BaSi) were conducted in 0.1 M [EMIM][2-CNpyr]/acetonitrile electrolyte with 0.1 M TEAP supporting salt in a T-cell with the three-electrode setup described above. The cell was placed in a Faraday's cage on an isolating surface (i.e., a sponge) to avoid any external disturbances on the electrochemical signal collected from microvoltammetry (e.g., external electromagnetic fields or vibrations present in the lab environment). Prior to the experiments, the microelectrode was sonicated in acetonitrile solution for 5 min to ensure a clean surface.

Dynamic Impedance. The double layer capacitance was dynamically measured by using dynamic electrochemical impedance spectroscopy (DEIS). The instrumentation details and the experimental setup have been described previously,⁴² and only a brief description is given here. A multisine waveform consisting of 45 frequencies between 37.5 kHz and 1 Hz was synthesized by a waveform generator. Briefly, (1) each frequency in the waveform had an integer number of periods in the waveform period, $T = 1/f_{\text{min}}$; (2) frequencies are based on Popkirov's prime number selection rule that is then multiplied by f_{min} to reduce harmonic and interharmonic overlap; (3) the amplitude for individual waves decreased by half for every decade increase in the frequency; (4) the phases of individual waves were randomized; and (5) the maximum amplitude of the ac waveform was ~ 35 mV. The waveform was fed into a Biologic potentiostat (SP-240) and was added atop the cyclic voltammogram protocol. After measurement, the raw data was transformed into the frequency domain using a sliding fast Fourier transform algorithm, which was then converted to complex impedance (Z) via eq 1:

$$Z = \frac{(E_r I_r + E_i I_i) + i(E_i I_r - E_r I_i)}{(I_r^2 + I_i^2)} \quad (1)$$

where E stands for potential, I stands for current, and r and i are for real and imaginary, respectively. We extracted only the frequencies that correspond to those used in the multisine waveform that was applied to the system. We only fit frequencies between 0.1 and 37.5 kHz to a standard Randel's circuit to extract the double layer capacitance value. For these measurements, the cell was a 1/4 in. T-cell with a 2 mm Ag CH instrument working electrode and 1/4 in. diameter polished graphite counter electrode and a Ag/AgCl reference electrode.

H-Cell Electrolysis. The bulk electrolysis experiments were performed in a two-compartment H-type cell separated by a Nafion-117 cation exchange membrane (Fuel Cell Store, USA) (Figure 1b). The cathodic chamber contained the working electrode (Ag foil, $\geq 99.9\%$, area, 0.44 cm^2 , thickness 1.0 mm, supplied by BeanTown Chemical) and the same reference electrode (Ag/Ag⁺) described previously for LSVs. The anodic chamber housed the counter electrode: Pt mesh (99.9%, 2×2 cm, BASi Research Products) or carbon rod (6 mm dia., BASi Research Products). The distance between working and counter electrodes was 5 cm. The working electrode chamber was continuously stirred, and CO₂ gas (10 sccm) was fed through the overhead of the catholyte chamber to ensure sufficient CO₂ availability in the electrolyte. It should be noted that bubbling of CO₂ through the catholyte was avoided since it could lead to uneven flow at the H-cell outlet, potentially resulting in incorrect interpretations when calculating the product selectivity. The gaseous products sampled from the overhead of the catholyte chamber were analyzed with the online gas chromatography (GC) (Agilent, 7890B) equipped with a flame ionization detector (FID) and thermal conductivity detector (TCD). The liquid product was analyzed by ¹H and ¹³C NMR spectroscopy after electrolysis. Since most of the H-cell electrolysis experiments were performed with 0.1 M IL concentration, NMR samples were prepared by mixing 350 μL

of DMSO-*d*₆ solvent with 350 μL of electrolyte. In the case of pure IL NMR sampling, only 30 μL of IL in 720 μL of DMSO-*d*₆ solvent was used for NMR quantification.

The Faradaic efficiency (FE) for ECO₂R gaseous products during the electrolysis experiments was calculated as follows (eq 2):⁴³

$$\text{FE}(\%) = \frac{e_{\text{output}}}{e_{\text{input}}} \times 100 = \frac{(V/V_m)YN}{(V/v)It/F} \times 100 \quad (2)$$

where e_{output} is the number of electrons required for ECO₂R, e_{input} is the number of electrons measured during the sampling period, V is the volume of GC sampling loop (mL) (0.25 mL for CO and 0.1 mL for H₂), V_m is the ideal molar gas volume (22.4 L/mol), N (=2) is the number of electrons required to form CO or H₂ (possible ECO₂R products with the Ag electrode), F is the Faraday constant (96,485 C/mol), and I is the recorded current. The flow rate of CO₂ was $v = 10$ mL/min. The measured amount of product (Y in units of mol) in a 0.25 mL sample loop was then calculated using the corresponding calibration curves of the GC that were previously developed using standard gases.¹²

Ionic Conductivity and Viscosity Measurements. Ionic conductivity (σ) measurements were performed using electrochemical impedance spectroscopy (EIS).⁴⁴ Two platinized platinum electrodes (BioLogic USA) were immersed in a sample solution, and impedance measurements were performed at 100 Hz to 100 kHz with 5 mV voltage amplitude at 25 ± 0.2 °C. The solution resistances of the samples were then determined from the intercept of the high frequency data with the real resistance axis in a Nyquist plot. Using the measured resistance, the conductivity was calculated using eq 3

$$\sigma(\text{mS} \cdot \text{cm}^{-1}) = \frac{k(\text{cm}^{-1})}{\rho(\text{ohm})} \times 10^3 \quad (3)$$

where σ is the ionic conductivity of the sample, k is the cell constant, and ρ is the solution resistance determined from the Nyquist plot. The cell constant of the platinized cell was measured with 0.1 M KCl before each measurement.

Viscosity measurements were performed with a microchannel viscometer (Rheosense; MicroVISC) in a temperature control unit maintained at 25 ± 0.2 °C. A single measurement required approximately 15 μL of sample. Before each sample was tested, the microchannel chip was rinsed with methanol followed by deionized water. The viscosities of N100 and S20 standards (supplied by Cannon Instrument Company) were measured at 25 ± 0.2 °C to confirm the reliability of measurements and found to be within 0.2%. Viscosity measurements were repeated three times, and an average is reported.

Electrochemical Characterization with Molecular Catalysts. Electrochemical techniques were performed using a Pine Wavedriver 10 bipotentiostat under an inert argon atmosphere, unless otherwise noted. All solutions were internally referenced to Fe(C₅H₅)₂⁺⁰. Electrolysis was performed in a custom H-cell with a gas bridge, with a 19 mL working compartment and 10 mL counter compartment separated by a porous glass frit with a gas bridge of 1 mL approximately. The working and counter compartments were sealed using GL25 and GL18 open top caps with silicone/PTFE septa from Ace Glass.

CV measurements with FeTPPS and Ni(cyclam)Cl₂ molecular catalysts were carried out with a 1 mm glassy carbon disk working electrode, a glassy carbon rod counter electrode, and a silver wire reference electrode. All CVs were scanned cathodically in a dry propylene carbonate solution containing 0.1 M [EMIM][2-CNpyr] and 0.1 M TBAPF₆ and 1 mM molecular catalyst when applicable. The electrodes have been scanned from the OCP up to -3.25 V vs Fe(C₅H₅)₂⁺⁰ with a scan rate of 100 mV/s. In the case of Ni(cyclam)Cl₂, a 5 mM stock solution of the compound in water was prepared. One ml of methanol was added to solubilize the catalyst. CVs with CO₂ were conducted by sparging solvent-saturated CO₂ into the electrolyte for 10 min. Controlled potential electrolysis experiments were performed in a custom H-cell with a 16 mL working

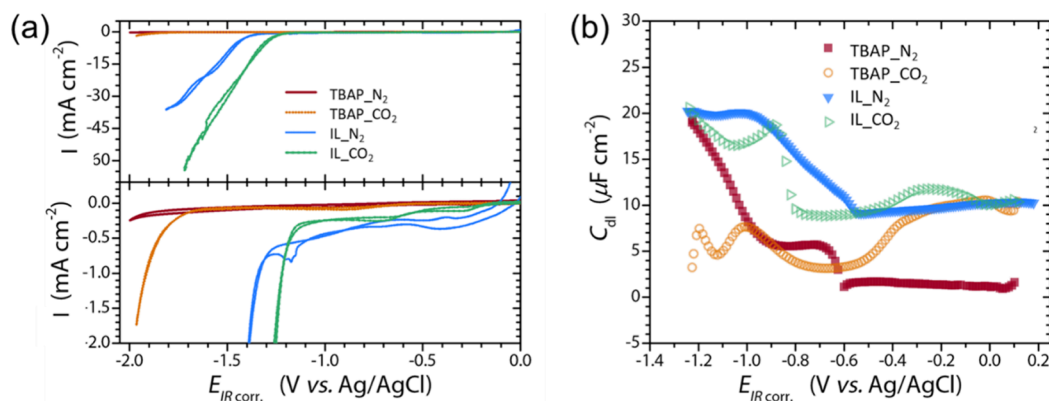


Figure 2. (a) CV curves recorded with the Ag working electrode in N_2 and CO_2 saturated electrolytes containing 0.1 M TBAP/acetonitrile (red and orange) and 0.1 M [EMIM][2-CNpyr] added to 0.1 M TBAP/acetonitrile (blue and green) (CV scan rate: 10 mV/s). (b) Differential capacitance curves obtained by fitting the time-resolved impedance data to a Randles circuit to the higher frequency range (0.1 to 37.5 kHz).

compartment separated from an 8 mL counter compartment by a porous glass frit. The working and counter compartments were sealed using GL25 and GL18 open top caps with silicone/PTFE septa from Ace Glass. The working compartment containing the catholyte consisted of 1 mM molecular catalyst, 0.1 M IL, and 0.1 M TBAPF₆ in propylene carbonate. The counter compartment containing the anolyte had 0.1 M TBAPF₆ in propylene carbonate. For Fe(TPPS), the catholyte additionally included 0.1 M TFE as the proton source. For Ni(cyclam)Cl₂, the catholyte additionally included methanol (1.0 mL in the total of 10 mL catholyte) and water (1.8 mL in the total of 10 mL catholyte) as the proton source. Both systems used excess Fe(C₅H₅)₂ in the anolyte as a sacrificial reductant. The working electrodes were a 7/8 in. × 2.5 in. piece of carbon cloth purchased from Fuel Cell Earth. The reference electrode was a jacketed Ag^{+/0} wire containing an electrolyte solution of 0.1 M TBAPF₆ in propylene carbonate. The counter electrode used the same carbon cloth as the working electrode in the case of Fe(TPPS) and nichrome wire in the case of the Ni(cyclam)Cl₂ system, separated from the bulk solution by a porous Vycor frit. A Restek A-2 Luer lock gastight syringe was used to sample the headspace of the working compartment. Products were quantified using an Agilent 7890B GC instrument with a HP-PLOT molecular sieve column (19095P-MS6, 30 m × 0.530 mm, 25 μ m) and thermal conductivity detector under helium carrier gas.

RESULTS AND DISCUSSION

Considerations for IL Synthesis. As the halide impurity of the electrolyte is critical in electrochemical studies, careful monitoring of [EMIM][Br] conversion to [EMIM][OH] was performed by characterizing the solution after it passed through the anion exchange column by NMR (Figure S2), FTIR (Figure S3), and ion chromatography for halide content. Other considerations besides the minimization of halide impurity were the reaction time and the reactant stoichiometry. It was found that the reaction is fast and completes within 1 h regardless of the batch sizes synthesized (6 and 40gr). As for the reaction stoichiometry, it is common that one of the reagents is introduced in slight excess to push the equilibrium toward the synthesis products. However, this practice requires elevating the heating temperature under vacuum which can result in color change in the IL, attributed to possible degradation.⁴⁵ As confirmed from the NMR analysis of the syntheses with varying reactant compositions (Figure S4a) and halide salts (Figure S4b), the best composition was confirmed to be equimolar starting materials, irrespective of the halide when using the same anion exchange resin.

Considerations for Electrochemical Characterization of IL Electrolytes. *Probing of the Electrode–Electrolyte*

Interface through Capacitance. Dynamic electrochemical impedance spectroscopy is a powerful tool that follows the evolving nature of electron transfer processes and double layer capacitance at charged interfaces. The impedance evolution during CO_2 electroreduction is outside the scope of this section; rather, we will focus on the differential capacitance before active catalysis. Capacitance holds information on how the electrolyte–electrode interphase is structured and restructures with applied potential and of course the chemical structure of the catalyst surface governs electrocatalytic activity. Figure 2 shows the apparent catalytic activity of Ag with and without [EMIM][2-CNpyr] present as well as the capacitance obtained from DEIS. The corresponding capacitance curves show a drastic increase in C_{dl} value upon IL addition. This is to be expected as tetrabutylammonium (TBA) cations do not densely adsorb at charged interfaces,^{46–48} resulting in low surface capacitance on the order of 2–5 μF cm⁻². However, [EMIM] cations can reorient themselves to increase surface charge.⁴⁹ Here, the addition of the IL increases C_{dl} at potentials more positive than -0.6 V vs Ag/AgCl from 2 to 10 μF cm⁻². We note that these results are different from standard differential capacitance measurements as they are not at a steady state. The potential is actively sweeping, which prevents cations from crowding and increasing the double layer thickness, thus resulting in increased C_{dl} values than expected. In the case of crowding effects, CO_2 mass transport to the surface may also experience hindrance due to the thickening of the interface by [EMIM]⁺ species.

CO_2 saturation further affects the C_{dl} profile more negative than -0.6 V vs Ag/AgCl with and without the IL. Focusing on the potential range between -0.8 and -1.2 V when IL is present, the C_{dl} increase is delayed, shifting from -0.56 V in N_2 sat. to -0.79 V in CO_2 sat. V vs Ag/AgCl. This result suggests that positive charges are blocked from the surface and indicative of adsorbed intermediates or spectators, which are then removed through sweeping in a more negative direction. From NMR (Figure S5), we see CO_2 adducts of both [EMIM]⁺- CO_2 ⁻ and [2-CNpyr]- CO_2 . These species were observed via surface-enhanced Raman spectroscopy adsorbed onto the Cu catalyst.¹³ Given that [EMIM]⁺- CO_2 ⁻ is a neutral species, it is likely that this specie is what impedes the capacitance, and its dynamic reorientation and reduction result in a sharp capacitance increase.

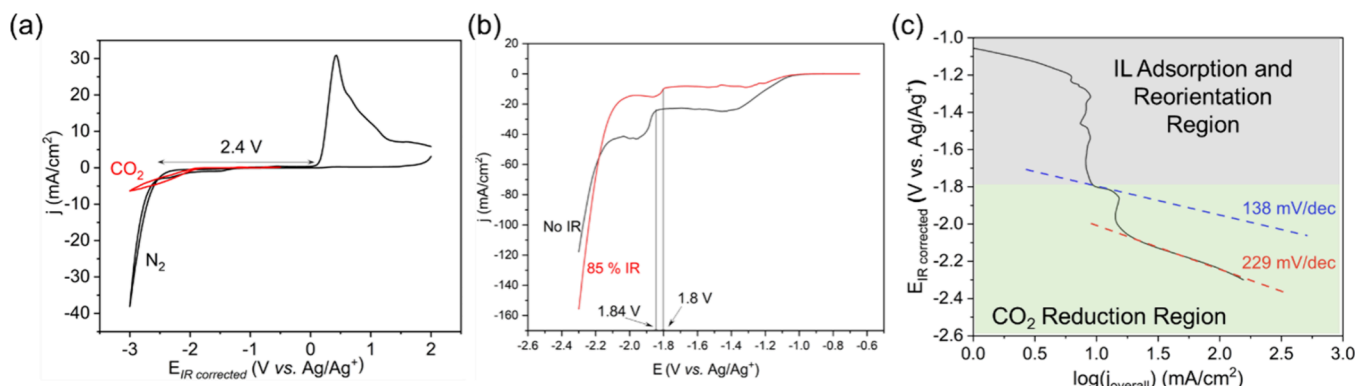


Figure 3. (a) Cyclic voltammetry of [EMIM][2-CNpyr] under N_2 (black) and CO_2 (red) sat. on the Ag disk electrode (1.5 mm dia) with a scan rate of 10 mV/s, recorded using a T-cell. The electrochemical window of 2.4 V was determined using a cutoff current density of 2 mA/cm². (b) LSV of CO_2 saturated 0.1 M [EMIM][2-CNpyr]/acetonitrile with 0.1 M TEAP supporting salt recorded using a T-cell with the Ag microelectrode (12.5 μ m). The red and black curves represent LSV measurement performed with and without IR correction, showing a positive shift in the ECO_2R onset potential after IR compensation. (c) Tafel plot of ECO_2R in CO_2 saturated 0.1 M [EMIM][2-CNpyr]/acetonitrile with 0.1 M TEAP supporting salt. The Tafel plot is derived from the LSV measurement performed with the Ag microelectrode with 85% IR correction as shown in the panel.

Establishing the Electrochemical Stability and ECO_2R Onset Potential. ILs designed for specific applications such as ECO_2R are often synthesized in laboratories in very small quantities. Therefore, the initial assessment of their application performance and screening for a systematic set of structures necessitate the minimization of sample volume. For determining the electrochemical stability window, a T-cell setup has been used by many researchers^{41,44,50} due to its microliter-sized sample requirement and ease of control in the environmental gas. Figure 3a shows the cyclic voltammograms obtained for [EMIM][2-CNpyr] by the T-cell shown in Figure 1a. It has been reported that the electrochemical stability window of ILs is constrained by the reduction potential of the cations and the oxidation potential of the anions. As shown in Figure 3a, an exponential increase in the cathodic current was observed from -2.3 V (vs Ag/Ag⁺) under N_2 , which can be attributed to the extensive reductive degradation of [EMIM][2-CNpyr]. Additionally, the oxidation peak at 0.5 V is observed, which is mainly associated with pyrrolide anion oxidation.⁵¹ In comparison, CO_2 -saturated [EMIM][2-CNpyr] showed a very low current response, indicating an increased mass transport limitation due to the viscosity increase from 68 to 247 cP at 25 °C after CO_2 exposure.³⁶ This viscosity increase is a result of the interaction of the α -carbon on the imidazolium with CO_2 through the acidic hydrogen, as reported previously.¹¹ This is an important aspect of reactive ILs and necessitates proper IR correction⁵² for not only an initial assessment on electrochemical stability windows but also the onset potential for electron transfer reactions.

Even though the use of microelectrodes reduces the effect of diffusion limitations by changing the diffusion mode from linear to spherical and thereby reducing the ohmic drop,⁵³ IR correction is still important. Figure 3b exemplifies the utilization of IR correction with a microelectrode for the ECO_2R in a diluted IL electrolyte. Compensation for voltage drops is done by potentiostat by applying a high frequency ac perturbation (e.g., 100 kHz), which enables the measurement of only the uncompensated solution resistance. Correction allows for more accurate determination of the potential at the microelectrode–electrolyte interface. As shown in Figure 3b, the ECO_2R onset was observed at -1.85 V with no IR

correction, and it shifts to -1.82 V after 85% IR correction. Even though the potential shift is relatively small for the diluted electrolyte, the effect becomes more prominent with concentrated electrolytes or neat ILs. Another important aspect is the shielding that is needed against external factors such as mechanical vibration and electrical noise present in the lab environment. Thus, the electrochemical cells equipped with microelectrodes should be placed inside a Faraday cage for prevention against external electromagnetic interferences that can distort the electrochemical signals (see Figure S6 for the impact of using a Faradaic cage).

Examination of Kinetics, Solvent Effects, and Product Selectivity. Similar to the difficulty in determining the onset potential, the investigation of electron transfer kinetics is not straightforward with reactive ILs such as [EMIM][2-CNpyr]. It is known that ILs alter the electrode–electrolyte interfaces and form a unique double layer,⁵⁴ and reactive IL systems further present a dynamic behavior where species distribution varies according to the absorption and consumption rates of CO_2 . Therefore, it is not possible to determine which species are being reduced at each potential, leading to limited linearity in Tafel slopes. Figure 3c shows an exemplary Tafel plot for [EMIM][2-CNpyr] obtained by microelectrode voltammetry. Throughout the polarization of the interface, IL cations adsorb on the electrode surface and change their orientation and lateral organization on the electrode surface,¹³ which causes small current responses. In the ECO_2R region, the reduction starts with a Tafel slope of 138 mV/decade, and the slope further increases to 229 mV/decade. This high value may suggest mass transport limitation or may be an indication of a small symmetry factor,⁵⁵ which is related to a large reorganizational energy penalty due to reduction reaction on the electrode. It is worth noting that the changes in Tafel slope occur within a very short potential window (i.e., 200 mV), as seen in Figure 3c, and the regions for the change in electrochemical reactions are distinct and better seen in Figure 3b. These adsorption and double layer reorganization regions may not be distinguishable with macroelectrodes with large dispersion of electric field lines and catalytic sites, thus requiring careful analysis to relate observed kinetics between macro- and microelectrodes.

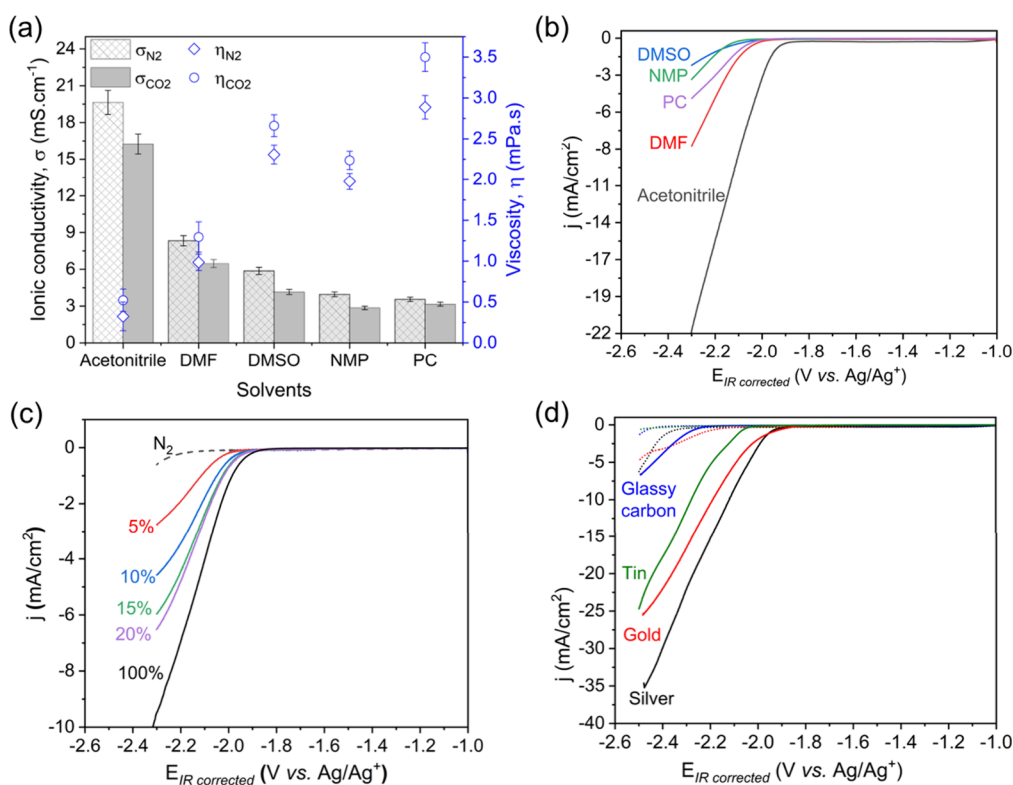


Figure 4. (a) Ionic conductivity (columns) and viscosity (circles) of 0.1 M IL electrolyte with various diluents/cosolvents at 25 °C: with N₂ (hollow) or CO₂ (filled) saturation. (b) LSVs with the Ag electrode under a CO₂ atmosphere. (c) LSV recorded with the Ag disk working electrode showing the effect of CO₂ partial pressure in feed gas on ECO₂R. (d) LSV of the glassy carbon, gold, silver, and tin electrodes in N₂ (dotted line) and CO₂ (solid line) saturated 0.1 M [EMIM][2-CNpyr] showing the effect of electrode material on CO₂ reduction activity. LSVs were recorded in a single compartment electrochemical cell (electrolyte volume, 5 mL) at 10 mV/s scan rate and electrolyte solutions composed of 0.1 M [EMIM][2-CNpyr] added to 0.1 M TEAP (supporting salt) in respective solvents.

In addition to the kinetics, it is of interest to examine the product selectivity of the reduction reaction. Appreciable amounts are needed to reliably identify and quantify the products, which require a high electrolyte conductivity to facilitate high currents. To overcome the high viscosity of ILs and achieve high currents, dilution is required.^{3,41} Water as a dilutant introduces HER as a side reaction and lowers the Faradaic efficiency (FE) toward ECO₂R products.⁵⁶ Moreover, water can lead to bicarbonate formation upon CO₂ exposure,^{11,36} which shifts effective pH and ultimately increases additional H₂ evolution during ECO₂R.² Therefore, we examined aprotic organic solvents and their effects on viscosity, conductivity, and the resulting current responses to identify suitable diluents/cosolvents for reactive ILs for reliable characterization of ECO₂R products as it has been shown that electrolyte effects are significant in ECO₂R.^{34,57}

Figure 4a shows how the viscosity and conductivity and the corresponding LSVs in Figure 4b show that the choice of solvent significantly influences the CO₂ reduction onset potential as well as the resulting CO₂ electroreduction activity. This difference can be attributed to several factors: the ohmic drop induced by the lower ionic conductivity of electrolyte solutions composed of DMF (6.47 mS·cm⁻¹), DMSO (4.15 mS·cm⁻¹), NMP (2.85 mS·cm⁻¹), and PC (3.16 mS·cm⁻¹), which is a factor of 2 to 4 smaller than the acetonitrile-based electrolyte (16.25 mS·cm⁻¹) (Figure 4b);^{34,57} effective CO₂ concentration (presented in Table 1), which includes speciation energetics and subsequent electrochemical activa-

tion; lastly, CO₂ diffusion, which is governed by electrolyte viscosity.

While dilution is effective in enhancing ECO₂R rates, it is important to establish that the IL is still effective in terms of maintaining a high CO₂ solubility even when diluted. For physically absorbing ILs, the advantage of high CO₂ solubility is most likely lost when diluted, especially under low partial pressures of CO₂. However, reactive ILs present superior CO₂ capacities due to chemisorption. Figure S5 shows the quantitative ¹³C NMR spectra of 0.1 and 1.5 M [EMIM][2-CNpyr] in acetonitrile, in comparison to the neat [EMIM][2-CNpyr] under N₂ and CO₂ saturation. It is determined that the same reaction products are present in both the diluted and neat samples, thus demonstrating the effectiveness of the CO₂-reactive IL even under dilution. The consideration for the right IL concentration should be based on the CO₂ source as much as the transport properties.^{12,13,16} For instance, a higher IL concentration (e.g., 1.5 M for a significant concentration of complexation sites) is suitable for a low partial pressure of CO₂ and vice versa (e.g., 0.1 M for enhanced transport properties). Figure 4c shows the attainable current responses using a Ag electrode with 0.1 M IL in acetonitrile and 0.1 M tetrabutylammonium perchlorate (TEAP) as the supporting electrolyte as a function of the CO₂ percentage in the feed gas (balanced with N₂). Controlling the partial pressure of CO₂ allows us to change the CO₂ concentration in the bulk electrolyte at room temperature.³⁶ As seen, increasing the CO₂ partial pressure leads to a shift in onset potential and increase in current density, capturing the expected relationship between

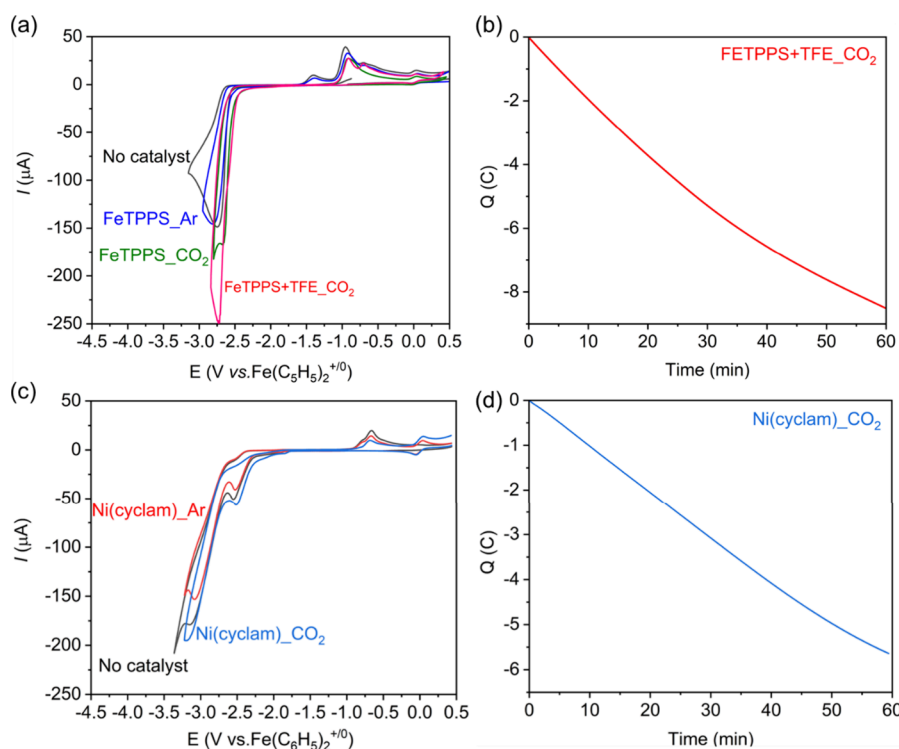


Figure 5. (a) CV data of 0.1 M [EMIM][2-CNpyr] in propylene carbonate (black) with 1 mM FeTPPS (blue). Saturation of CO₂ (green) and addition of 0.1 M TFE (red) result in a shift in the onset potential of [EMIM][2-CNpyr] reduction. (b) Controlled potential electrolysis of 1 mM FeTPPS with 0.1 M [EMIM][2-CNpyr] and 0.1 M TFE in propylene carbonate. (c) CV response of 0.1 M [EMIM][2-CNpyr] in propylene carbonate:water and methanol (red trace), with the addition of Ni(cyclam)²⁺ at 1 mM (blue trace). Solution was saturated with CO₂ resulting in the current enhancement (green trace). All the CVs were recorded at 100 mV/s. (d) CPE data showing the charge vs time plot with a potential held at -2.62 V vs Fc^{+/0} under the same conditions as cyclic voltammograms.

the ECO₂R and the concentration of CO₂ in the electrolyte as it directly affects the near-surface concentration of CO₂.⁵⁸

Finally, the effect of the heterogeneous electrocatalyst was investigated in terms of the onset potential and current response for ECO₂R. Figure 4d shows the LSVs with Ag, Au, Sn, and glassy carbon (GC) electrodes in 0.1 M [EMIM][2-CNpyr] in acetonitrile with TEAP supporting salt, under N₂ and CO₂ purging conditions. In the N₂-purged electrolyte (indicated by the dashed line), the onset potentials for the cathodic reaction were around -2.45 , -2.3 , -2.05 , and -2.1 V vs Ag/Ag⁺ on glassy carbon electrodes, Ag, Sn, and Au, respectively. The majority of the reduction current was attributed to the degradation of [EMIM][2-CNpyr] itself, and the onset potential for the IL degradation varied, depending on the electrode material. However, when the electrolyte was purged with CO₂ (illustrated by the solid line), the onset potential shifted toward more positive values: -2.25 V vs Ag/Ag⁺ on GC, -2.04 V vs Ag/Ag⁺ on Sn, and -1.89 V vs Ag/Ag⁺ on Ag and Au electrodes, respectively. This result suggests that the CO₂ reduction activity on the GC electrode is relatively low compared to Sn, Au, and Ag, thus confirming the heterogeneous catalysis with the metal electrodes. The CO₂ reduction onset potentials observed for Ag and Au are the same; however, a higher ECO₂R current was observed from -1.9 to -2.3 V (vs Ag/Ag⁺) with the Ag electrode, indicating superior activity compared to Au. Because of high selectivity of CO on Ag, bulk electrolysis experiments were performed with the Ag electrode in the following section.

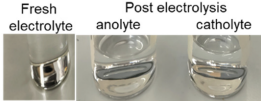
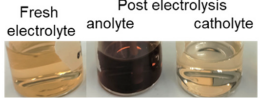
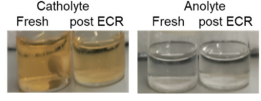
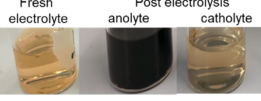

ECO₂R activity was also studied in the presence of the molecular catalyst FeTPPS. Similar to the heterogeneous

conditions described above, CV data of FeTPPS with 0.1 M [EMIM][2-CNpyr] in propylene carbonate shows an anodic shift in onset potential when purged with CO₂ (Figure 5a). Controlled potential electrolysis of this system at -2.5 V versus Fe(C₅H₅)₂^{+/0} with 0.1 M TFE as a proton donor resulted in a linear increase in charge with time, passing -8.5 C of charge in 1 h (Figure 5b). The electrolysis exclusively produced CO with an FE of 100%.

Figure 5c shows the cyclic voltammogram recorded in IL 0.1 M [EMIM][2-CNpyr] and 1 mM Ni(cyclam)²⁺. The addition of CO₂ in the presence of water and methanol shows a decrease in the cathodic potential with a simultaneous enhancement in the current, showing its catalytic activity for CO₂ reduction. CPE measurements carried out with a potential at -2.62 V vs Fe(C₅H₅)₂^{+/0} under similar conditions showed linear accumulation of charge over time (Figure 5d). The gas product analysis of the headspace of the H-cell with a gas bridge showed HER and CO products with FE values of 14 and 79%, respectively.

Discussions on the Choice of the Reference Electrode. Accurate and reproducible electrochemical measurements require well-defined and stable reference electrodes. However, most conventional reference electrodes are designed for aqueous systems, containing high concentrations of water and chloride.⁵⁹ In nonaqueous electrolysis studies, even trace amounts of water and chlorides can significantly impact electrochemical performance. Consequently, these reference electrodes are unsuitable for nonaqueous systems.⁶⁰ These findings have given rise to three main classes of reference electrodes used in nonaqueous media: pseudo, double

Table 2. Experimental Conditions of the Performed H-cell Electrolysis Used to Investigate the Effect of Electrode Materials and Electrolyte on Product Distribution and Electrochemical Stability^a

#	Cathodic chamber		Anodic chamber			Q (C)	Remarks
	Electrode	Electrolyte	Electrode	Electrolyte	Feed gas		
1	Ag	0.1 M TEAP	Pt	0.1 M TEAP	CO ₂	2.18	
2	Ag	0.1 M IL	Pt	0.1 M IL	N ₂	12.4	
3				0.2 M TEAP	CO ₂	12	
4	Ag	0.1 M IL	Carbon rod	0.1 M IL	CO ₂	6.73	
5			Pt	0.1 M 2-CNpyrH		12.3	 <p>no color change with catholyte</p>
6			Pt	0.1 M H ₂ SO ₄		12.6	no color change with catholyte

^aTotal charge (Q) is reported for 60 min of electrolysis at -2.1 V (vs Ag/Ag⁺). Feed gas was consistently at 10 mL/min for both compartments. Cathodic chamber feed gas was CO₂ in all cases. Pictures in the last column show the change in electrolyte color before and after electrolysis.

junction, and soluble redox pairs⁶¹ (see Figure S7). In many studies involving ILs, researchers have resorted to using “quasi-reference” or “pseudoreference” electrodes. In these cases, a silver or a platinum wire is immersed in the bulk electrolyte. Advantages of using these reference electrodes include decreased ohmic resistance, a negligible liquid junction potential, no contamination of solvent molecules or ions that an aqueous reference electrode might transfer, and no potential for frit pore plugging. However, these electrodes are often unreliable because their potential is influenced by impurities in the ILs or traces of oxides and other electrochemically active compounds on the electrode surface. Consequently, the reference potential can vary depending on the analyte, primarily due to differences in impurity solubilities and the oxide compound presence. Even within the same sample, the potential can drift over time, especially after cleaning and polishing the pseudoreference electrode.

The next class of reference electrodes involves the use of soluble redox pairs; this type of reference electrode is commonly used in aqueous media and includes Ag/AgCl and SCE.⁶² These electrodes include a glass tube with a mounted frit that separates the redox pair from the main chamber of the cell. To modify these electrodes for use in nonaqueous media, the solution within the reference electrode should be the same as the electrolyte in the cell with the addition of the desired redox pair. Advantages of using these types of reference electrodes are specifically the elimination of water contamination as well as a liquid junction potential. The

main disadvantage to this class of reference electrodes is finding soluble and stable redox pairs in organic solvents. A redox pair that is frequently used in nonaqueous chemistry, especially within the field of ILs, is the silver–silver ion (Ag/Ag⁺) electrode. It can be prepared by immersing a clean Ag wire into a solution containing 10 mM silver nitrate dissolved in 0.1 M tetraalkylammonium salts in acetonitrile.

Silver nitrate is soluble in a variety of organic solvents, and the filling solution to the reference electrode should be constituted of the same solvent and electrolyte salt to avoid liquid junction potentials and ion contamination. It is important to note that this reference electrode is still susceptible to instabilities, and proper maintenance of electrodes is key to reproducibility. It should be further noted that the reference potential of Ag/Ag⁺ is strongly affected by the presence of trace amounts of water and the type of solvent used as it changes the solvation of Ag⁺ ion.⁶¹ Therefore, a molecule with well-defined electrochemical behavior, such as ferrocene, can be added in very small amounts to the bulk electrolyte as an internal reference.⁶³ The representative CV of Fc/Fc⁺ redox behavior on the Pt electrode is shown in Figure S8. However, issues can arise when the addition of internal reference redox couples leads to contamination of the working electrode, particularly when the redox potentials of the working electrode material and reference redox couples are closely aligned. This is particularly true in the case of Ag working electrode and the Fc/Fc⁺ redox couple.¹⁶ Further, other issues related to reference electrode

frit pore plugging (Figure S9) and Ag^+ ion leakage⁶⁴ are reported, which interfere with the stability of reference electrode.⁶⁵ These interferences can be minimized by using a double junction or salt bridge during the measurements (as shown in Figure S7). However, a high electrode impedance due to the double junction needs to be accounted during the measurements.

Approach to H-Cell Electrolysis for ECO_2R with IL Electrolytes and Interpretation of Results. The methods described above are appropriate for screening of ILs and initial assessment of ECO_2R . However, these methods alone are not sufficient for a further understanding of reaction products, Faradaic efficiencies, and practical electrolyte stability. To decouple the interfacial reactions (e.g., ECO_2R vs electrolyte degradation) at anode and cathode surfaces, the best next step is to perform an H-cell electrolysis experiment. In an H-cell where the anolyte and catholyte compartments were separated by a pretreated Nafion-117 membrane, electrolysis experiments were performed at -2.1 V (vs Ag/Ag^+) for 1 h with different combinations of electrode materials, electrolytes, and feed gases as summarized in Table 2. The resultant chronoamperometric curves are shown in Figure S10. These experiments were planned to study the effect of the counter electrode material, electrolyte composition, and IL degradation on ECO_2R performance.

To investigate the electrolyte composition, we initially performed electrolysis experiments with the use of 0.1 M TEAP/acetoneitrile as the electrolyte in both compartments, which resulted in 2.18 C charge utilization at -2.1 V (vs Ag/Ag^+) in 1 h of ECO_2R over the Ag electrode. However, under the same experimental conditions, with the addition of 0.1 M IL, a 6-fold increase in total charge utilization was observed. In both cases, only CO was detected in the gaseous product with a Faradaic efficiency exceeding 95%. This increase in charge utilization can be attributed to the increased availability of CO_2 and the stabilization of reaction intermediates by the imidazolium cation.¹² To further investigate the changes occurring in the anolyte and catholyte, electrolytes were analyzed postelectrolysis using ^1H NMR spectroscopy and no changes were observed in the catholyte (Figure S11). Note that NMR is effective for measuring compounds that are 1 wt % or higher in the liquid sample prepared. However, a few new peaks were detected in the anolyte (Figure S12), confirming the oxidative degradation of the IL at the Pt anode surface. Additionally, we observed a change in the color of the anolyte from light yellow to dark brown (as shown in Figure S12). Surprisingly, a similar anolyte degradation was observed when a carbon rod anode was used, which is typically considered inactive for most electrochemical reactions. The appearance of new peaks in the ^1H NMR spectrum is attributed to the oxidative degradation (highlighted by the red arrow in Figure S12). The oxidative degradation of pyrrole compounds under the same applied potentials has been reported in the literature.⁵¹ To further validate our findings, we performed an electrolysis experiment with the addition of 0.1 M 2-CNpyrH to the anode compartment. The same color change was observed, thus pointing to the similarity of the pyrrole species decomposition. Thermal degradation of [EMIM][2-CNpyr] was examined before, and the dimerization of the anion along with H_2 release was reported in addition to the ring opening of the cation.⁴⁵ A similar mechanism could influence the color change observed here. As the degradation products could crossover during long-term electrolysis studies,

we conclude that IL should be avoided in the anolyte, especially when the IL contains a nucleophilic anion.

Most H-cell electrolysis experiments reported in the literature utilize aqueous anolyte solutions. Therefore, ECO_2R activity in the presence of 0.1 M H_2SO_4 on the anode side and nonaqueous 0.1 M [EMIM][2-CNpyr] on the cathode side was examined at -2.1 V vs Ag/Ag^+ on the Ag electrode. We observed a continuous increase in the current over time. This was attributed to the exchange of H^+ from the anolyte to the catholyte, resulting in excess HER. Gas product analysis confirmed H_2 evolution: the initially observed Faradaic efficiency for CO was 92% (over 20 min) decreased to 78% after 60 min (Figure S13). Hence, our findings highlight the importance of investigating the appropriate anolyte solution when employing the IL as the active catholyte component in the combined capture and electrochemical conversion of CO_2 .

CONCLUSIONS

An improved method of bulk synthesis of imidazolium cyanopyrrolide IL is presented in consideration of precursor composition and reaction for electrochemical studies. This refinement enhances the efficiency of scalable IL synthesis with a minimized impurity. Furthermore, important considerations for studying homogeneous and heterogeneous electrocatalysis with ILs were discussed, using ECO_2R as a model reaction. The choices of catholyte solvent and the active electrode material have been shown to have a significant influence on the activation overpotential for CO_2 reduction. Further, oxidative degradation of ILs has also been observed, emphasizing the need to avoid ILs specifically composed of nucleophilic anions in the anolyte. This study presents key considerations when evaluating electrolytes for reactive capture and electrochemical conversion of CO_2 in particular, with nontraditional electrolytes containing functional ILs.

ASSOCIATED CONTENT

Supporting Information

The Supporting Information is available free of charge at <https://pubs.acs.org/doi/10.1021/acs.langmuir.3c03828>.

Details of IL synthesis; NMR and FTIR spectra; chronoamperometry curves; product analysis and selectivity data; photographs from the electrode (PDF)

AUTHOR INFORMATION

Corresponding Author

Burcu Gurkan – Department of Chemical and Biomolecular Engineering, Case Western Reserve University, Cleveland, Ohio 44106, United States; orcid.org/0000-0003-4886-3350; Email: beg23@case.edu

Authors

Saudagar Dongare – Department of Chemical and Biomolecular Engineering, Case Western Reserve University, Cleveland, Ohio 44106, United States; orcid.org/0000-0001-6782-0028

Oguz Kagan Coskun – Department of Chemical and Biomolecular Engineering, Case Western Reserve University, Cleveland, Ohio 44106, United States; orcid.org/0000-0002-8452-8552

Eda Cagli – Department of Chemical and Biomolecular Engineering, Case Western Reserve University, Cleveland, Ohio 44106, United States

Jared S. Stanley – Department of Chemistry, University of California, Irvine, California 92697, United States
Ab Qayoom Mir – Department of Chemistry, University of California, Irvine, California 92697, United States
Rowan S Brower – Department of Chemistry, University of California, Davis, California 95616, United States
Jesús M. Velázquez – Department of Chemistry, University of California, Davis, California 95616, United States;
orcid.org/0000-0003-2790-0976
Jenny Y. Yang – Department of Chemistry, University of California, Irvine, California 92697, United States;
orcid.org/0000-0002-9680-8260
Robert L Sacci – Chemical Sciences Division, Oak Ridge National Laboratory, Oak Ridge, Tennessee 37830, United States; orcid.org/0000-0002-0073-5221

Complete contact information is available at:
<https://pubs.acs.org/10.1021/acs.langmuir.3c03828>

Author Contributions

S.D. performed the electrochemical measurements, conducted the gas and liquid analysis, and analyzed the data. E.C. optimized the IL synthesis procedure. O.K.C. contributed to the electrochemical measurements with microvoltammetry. J.S.S., A.Q.M., and J.Y.Y. carried out the measurements and analysis with the molecular catalysts. R.S.B. and J.M.V. contributed to the discussions related to suitable reference electrodes. R.L.S. performed the dynamic electrochemical impedance spectroscopy measurements and analysis. B.G. conceived the project, conceptualized the study, and oversaw the progress. All the authors contributed to the discussions and edited.

Notes

The authors declare no competing financial interest.

ACKNOWLEDGMENTS

This study was funded by the U.S. Department of Energy, Office of Science, Basic Energy Sciences, Energy Frontier Research Centers, under the grant awarded to Center for Closing the Carbon Cycle (4C) (DE-SC0023427).

REFERENCES

- (1) Goyal, A.; Marcandalli, G.; Mints, V. A.; Koper, M. T. Competition between CO₂ reduction and hydrogen evolution on a gold electrode under well-defined mass transport conditions. *J. Am. Chem. Soc.* **2020**, *142* (9), 4154–4161.
- (2) de Salles Pupo, M. M.; Kortlever, R. Electrolyte effects on the electrochemical reduction of CO₂. *ChemPhysChem* **2019**, *20* (22), 2926–2935.
- (3) Sullivan, I.; Goryachev, A.; Digdaya, I. A.; Li, X.; Atwater, H. A.; Vermaas, D. A.; Xiang, C. Coupling electrochemical CO₂ conversion with CO₂ capture. *Nature Catalysis* **2021**, *4* (11), 952–958.
- (4) Rosen, B. A.; Salehi-Khojin, A.; Thorson, M. R.; Zhu, W.; Whipple, D. T.; Kenis, P. J.; Masel, R. I. Ionic liquid-mediated selective conversion of CO₂ to CO at low overpotentials. *Science* **2011**, *334* (6056), 643–644.
- (5) Lei, Z.; Chen, B.; Koo, Y. M.; MacFarlane, D. R. Introduction: Ionic Liquids. *Chem. Rev.* **2017**, *117* (10), 6633–6635.
- (6) Schubert, T. J. S., Current and future ionic liquid markets. In *Ionic liquids: current state and future directions*; ACS Publications: 2017; pp 35–65.
- (7) Gordon, C. M.; Muldoon, M. J.; Wagner, M.; Hilgers, C.; Davis, J. H. Jr.; Wasserscheid, P. Synthesis and Purification. *Ionic Liq. Synth.* **2007**, 7–55.
- (8) Seo, S.; Quiroz-Guzman, M.; DeSilva, M. A.; Lee, T. B.; Huang, Y.; Goodrich, B. F.; Schneider, W. F.; Brennecke, J. F. Chemically Tunable Ionic Liquids with Aprotic Heterocyclic Anion (AHA) for CO₂ Capture. *J. Phys. Chem. B* **2014**, *118* (21), 5740–5751.
- (9) Blundell, R. K.; Licence, P. Quaternary ammonium and phosphonium based ionic liquids: a comparison of common anions. *Phys. Chem. Chem. Phys.* **2014**, *16* (29), 15278–15288.
- (10) Lee, Y.-Y.; Gurkan, B. Graphene oxide reinforced facilitated transport membrane with poly(ionic liquid) and ionic liquid carriers for CO₂/N₂ separation. *J. Membr. Sci.* **2021**, *638*, No. 119652.
- (11) Lee, Y.-Y.; Edgehouse, K.; Klemm, A.; Mao, H.; Pentzer, E.; Gurkan, B. Capsules of reactive ionic liquids for selective capture of carbon dioxide at low concentrations. *ACS Appl. Mater. Interfaces* **2020**, *12* (16), 19184–19193.
- (12) Dongare, S.; Coskun, O. K.; Cagli, E.; Lee, K. Y.; Rao, G.; Britt, R. D.; Berben, L. A.; Gurkan, B. A Bifunctional Ionic Liquid for Capture and Electrochemical Conversion of CO₂ to CO over Silver. *ACS catalysis* **2023**, *13*, 7812–7821.
- (13) Coskun, O. K.; Dongare, S.; Doherty, B.; Klemm, A.; Tuckerman, M.; Gurkan, B. Tailoring Electrochemical CO₂ Reduction on Copper by Reactive Ionic Liquid and Native Hydrogen Bond Donors. *Angew. Chem., Int. Ed.* **2023**, *136*, No. e202312163.
- (14) Wang, Y.; Hatakeyama, M.; Ogata, K.; Wakabayashi, M.; Jin, F.; Nakamura, S. Activation of CO₂ by ionic liquid EMIM–BF₄ in the electrochemical system: A theoretical study. *Phys. Chem. Chem. Phys.* **2015**, *17* (36), 23521–23531.
- (15) Tanner, E. E.; Batchelor-McAuley, C.; Compton, R. G. Carbon dioxide reduction in room-temperature ionic liquids: the effect of the choice of electrode material, cation, and anion. *J. Phys. Chem. C* **2016**, *120* (46), 26442–26447.
- (16) Liu, B.; Guo, W.; Gebbie, M. A. Tuning Ionic Screening to Accelerate Electrochemical CO₂ Reduction in Ionic Liquid Electrolytes. *ACS Catal.* **2022**, *12* (15), 9706–9716.
- (17) Sun, L.; Ramesha, G. K.; Kamat, P. V.; Brennecke, J. F. Switching the reaction course of electrochemical CO₂ reduction with ionic liquids. *Langmuir* **2014**, *30* (21), 6302–6308.
- (18) Wuttig, A.; Surendranath, Y. Impurity ion complexation enhances carbon dioxide reduction catalysis. *ACS Catal.* **2015**, *5* (7), 4479–4484.
- (19) Ma, C.; Laaksonen, A.; Liu, C.; Lu, X.; Ji, X. The peculiar effect of water on ionic liquids and deep eutectic solvents. *Chem. Soc. Rev.* **2018**, *47* (23), 8685–8720.
- (20) Guo, W.; Liu, B.; Gebbie, M. A. Suppressing Co-Ion Generation via Cationic Proton Donors to Amplify Driving Forces for Electrochemical CO₂ Reduction. *J. Phys. Chem. C* **2023**, *127* (29), 14243–14254.
- (21) Figueiredo, M. C.; Ledezma-Yanez, I.; Koper, M. T. In situ spectroscopic study of CO₂ electroreduction at copper electrodes in acetonitrile. *ACS Catal.* **2016**, *6* (4), 2382–2392.
- (22) Jang, J.; Rüscher, M.; Winzely, M.; Morales-Guio, C. G. Gastight rotating cylinder electrode: Toward decoupling mass transport and intrinsic kinetics in electrocatalysis. *AIChE J.* **2022**, *68* (5), No. e17605.
- (23) Diercks, J. S.; Pribyl-Kranewitter, B.; Herranz, J.; Chauhan, P.; Faisnel, A.; Schmidt, T. J. An online gas chromatography cell setup for accurate CO₂-electroreduction product quantification. *J. Electrochem. Soc.* **2021**, *168* (6), No. 064504.
- (24) Wang, Y.; Hayashi, T.; He, D.; Li, Y.; Jin, F.; Nakamura, R. A reduced imidazolium cation layer serves as the active site for electrochemical carbon dioxide reduction. *Applied Catalysis B: Environmental* **2020**, *264*, No. 118495.
- (25) Pishgar, S.; Gulati, S.; Strain, J. M.; Liang, Y.; Mulvehill, M. C.; Spurgeon, J. M. In situ analytical techniques for the investigation of material stability and interface dynamics in electrocatalytic and photoelectrochemical applications. *Small Methods* **2021**, *5* (7), No. 2100322.
- (26) Iijima, G.; Kitagawa, T.; Katayama, A.; Inomata, T.; Yamaguchi, H.; Suzuki, K.; Hirata, K.; Hijikata, Y.; Ito, M.; Masuda, H. CO₂ Reduction Promoted by Imidazole Supported on a Phosphonium-

Type Ionic-Liquid-Modified Au Electrode at a Low Overpotential. *ACS Catal.* **2018**, *8* (3), 1990–2000.

(27) Katayama, Y.; Toshimitsu, Y.; Miura, T. Electrode kinetics of tris (2, 2'-bipyridine) ruthenium complexes in 1-ethyl-3-methylimidazolium tetrafluoroborate ionic liquid. *J. Electrochem. Soc.* **2013**, *160* (4), H224.

(28) Honores, J.; Quezada, D.; García, M.; Calfumán, K.; Muena, J.; Aguirre, M.; Arévalo, M.; Isaacs, M. Carbon neutral electrochemical conversion of carbon dioxide mediated by [M n+ (cyclam) Cl n](M= Ni 2+ and Co 3+) on mercury free electrodes and ionic liquids as reaction media. *Green Chem.* **2017**, *19* (4), 1155–1162.

(29) Grills, D. C.; Matsubara, Y.; Kuwahara, Y.; Golisz, S. R.; Kurtz, D. A.; Mello, B. A. Electrocatalytic CO₂ reduction with a homogeneous catalyst in ionic liquid: high catalytic activity at low overpotential. *J. Phys. Chem. Lett.* **2014**, *5* (11), 2033–2038.

(30) Froehlich, J. D.; Kubiak, C. P. Homogeneous CO₂ Reduction by Ni(cyclam) at a Glassy Carbon Electrode. *Inorg. Chem.* **2012**, *51* (7), 3932–3934.

(31) Tarhini, A.; Aguirre-Araque, J.; Guyot, M.; Costentin, C.; Rogez, G.; Chardon-Noblat, S.; Prevot, V.; Mousty, C. Behavior of iron tetraphenylsulfonato porphyrin intercalated into LDH and LSH as materials for electrocatalytic applications. *Electrocatalysis* **2023**, *14* (1), 111–120.

(32) Gennaro, A.; Isse, A. A.; Vianello, E. Solubility and electrochemical determination of CO₂ in some dipolar aprotic solvents. *Journal of electroanalytical chemistry and interfacial electrochemistry* **1990**, *289* (1–2), 203–215.

(33) Lide, D. R. *CRC handbook of chemistry and physics*. CRC press: 2004; Vol. 85.

(34) Atifi, A.; Keane, T. P.; DiMeglio, J. L.; Pupillo, R. C.; Mullins, D. R.; Lutterman, D. A.; Rosenthal, J. Insights into the Composition and Function of a Bismuth-Based Catalyst for Reduction of CO₂ to CO. *J. Phys. Chem. C* **2019**, *123* (14), 9087–9095.

(35) Kumar, A. S.; Pupo, M.; Petrov, K. V.; Ramdin, M.; van Ommen, J. R.; de Jong, W.; Kortlever, R. A Quantitative Analysis of Electrochemical CO₂ Reduction on Copper in Organic Amide and Nitrile-Based Electrolytes. *J. Phys. Chem. C* **2023**, *127* (27), 12857–12866.

(36) Lee, Y.-Y.; Penley, D.; Klemm, A.; Dean, W.; Gurkan, B. Deep eutectic solvent formed by imidazolium cyanopyrrolide and ethylene glycol for reactive CO₂ separations. *ACS Sustainable Chem. Eng.* **2021**, *9* (3), 1090–1098.

(37) Kuwertz, R.; Kirstein, C.; Turek, T.; Kunz, U. Influence of acid pretreatment on ionic conductivity of Nafion® membranes. *J. Membr. Sci.* **2016**, *500*, 225–235.

(38) Gurkan, B.; Goodrich, B. F.; Mindrup, E. M.; Ficke, L. E.; Massel, M.; Seo, S.; Senftle, T. P.; Wu, H.; Glaser, M. F.; Shah, J. K.; Maginn, E. J.; Brennecke, J. F.; Schneider, W. F. Molecular design of high capacity, low viscosity, chemically tunable ionic liquids for CO₂ capture. *J. Phys. Chem. Lett.* **2010**, *1* (24), 3494–3499.

(39) McIntosh, A. J. S.; Griffith, J.; Gräsvik, J., Chapter 2 - Methods of Synthesis and Purification of Ionic Liquids. In *Application, Purification, and Recovery of Ionic Liquids*, Kuzmina, O.; Hallett, J. P., Eds. Elsevier: Amsterdam, 2016; pp 59–99.

(40) Hugar, K. M.; Kostalik, H. A. I. V.; Coates, G. W. Imidazolium Cations with Exceptional Alkaline Stability: A Systematic Study of Structure–Stability Relationships. *J. Am. Chem. Soc.* **2015**, *137* (27), 8730–8737.

(41) Schröder, U.; Wadhawan, J. D.; Compton, R. G.; Marken, F.; Suarez, P. A.; Consorti, C. S.; de Souza, R. F.; Dupont, J. Water-induced accelerated ion diffusion: voltammetric studies in 1-methyl-3-[2, 6-(S)-dimethylocten-2-yl] imidazolium tetrafluoroborate, 1-butyl-3-methylimidazolium tetrafluoroborate and hexafluorophosphate ionic liquids. *New J. Chem.* **2000**, *24* (12), 1009–1015.

(42) Sacci, R. L.; Seland, F.; Harrington, D. A. Dynamic electrochemical impedance spectroscopy, for electrocatalytic reactions. *Electrochim. Acta* **2014**, *131*, 13–19.

(43) Chen, C. S.; Handoko, A. D.; Wan, J. H.; Ma, L.; Ren, D.; Yeo, B. S. Stable and selective electrochemical reduction of carbon dioxide

to ethylene on copper mesocrystals. *Catalysis Science & Technology* **2015**, *5* (1), 161–168.

(44) Klein, J. M.; Squire, H.; Gurkan, B. Electroanalytical investigation of the electrode–electrolyte interface of quaternary ammonium ionic liquids: impact of alkyl chain length and ether functionality. *J. Phys. Chem. C* **2020**, *124* (10), 5613–5623.

(45) Lee, Y.-Y.; Cagli, E.; Klemm, A.; Park, Y.; Dikki, R.; Kidder, M. K.; Gurkan, B. Microwave Regeneration and Thermal and Oxidative Stability of Imidazolium Cyanopyrrolide Ionic Liquid for Direct Air Capture of Carbon Dioxide. *ChemSusChem* **2023**, *16*, No. e202300118.

(46) Han, T.; Park, M.-S.; Kim, J.; Kim, J. H.; Kim, K. The smallest quaternary ammonium salts with ether groups for high-performance electrochemical double layer capacitors. *Chemical Science* **2016**, *7* (3), 1791–1796.

(47) Koh, A. R.; Hwang, B.; Roh, K. C.; Kim, K. The effect of the ionic size of small quaternary ammonium BF₄ salts on electrochemical double layer capacitors. *Phys. Chem. Chem. Phys.* **2014**, *16* (29), 15146–15151.

(48) Katakura, S.; Nishi, N.; Kobayashi, K.; Amano, K.-i.; Sakka, T. Effect of Switching the Length of Alkyl Chains on Electric Double Layer Structure and Differential Capacitance at the Electrode Interface of Quaternary Ammonium-Based Ionic Liquids Studied Using Molecular Dynamics Simulation. *J. Phys. Chem. C* **2020**, *124* (14), 7873–7883.

(49) Klein, J. M.; Panichi, E.; Gurkan, B. Potential dependent capacitance of [EMIM][TFSI],[N 1114][TFSI] and [PYR 13][TFSI] ionic liquids on glassy carbon. *Phys. Chem. Chem. Phys.* **2019**, *21* (7), 3712–3720.

(50) Li, P.; Barnes, E. O.; Hardacre, C.; Compton, R. G. Microelectrode Voltammetry of Dioxygen Reduction in a Phosphonium Cation-Based Room-Temperature Ionic Liquid: Quantitative Studies. *J. Phys. Chem. C* **2015**, *119* (5), 2716–2726.

(51) Bozzini, B.; Bocchetta, P.; Alemán, B.; Amati, M.; Gianoncelli, A.; Gregoratti, L.; Sezen, H.; Taurino, A.; Kiskinova, M. Electrodeposition and pyrolysis of Mn/polypyrrole nanocomposites: a study based on soft X-ray absorption, fluorescence and photoelectron microspectroscopies. *Journal of Materials Chemistry A* **2015**, *3* (37), 19155–19167.

(52) Zheng, W. iR compensation for electrocatalysis studies: Considerations and recommendations. *ACS Energy Letters* **2023**, *8* (4), 1952–1958.

(53) Stulík, K.; Amatore, C.; Holub, K.; Marecek, V.; Kutner, W. Microelectrodes. Definitions, characterization, and applications (Technical report). *Pure Appl. Chem.* **2000**, *72* (8), 1483–92.

(54) Fedorov, M. V.; Kornyshev, A. A. Ionic Liquids at Electrified Interfaces. *Chem. Rev.* **2014**, *114* (5), 2978–3036.

(55) Gileadi, E.; Kirowa-Eisner, E. Some observations concerning the Tafel equation and its relevance to charge transfer in corrosion. *Corrosion science* **2005**, *47* (12), 3068–3085.

(56) Ganji, P.; Borse, R. A.; Xie, J.; Mohamed, A. G. A.; Wang, Y. Toward commercial carbon dioxide electrolysis. *Adv. Sustainable Syst.* **2020**, *4* (8), No. 2000096.

(57) König, M.; Vaes, J.; Klemm, E.; Pant, D. Solvents and supporting electrolytes in the electrocatalytic reduction of CO₂. *Iscience* **2019**, *19*, 135–160.

(58) Moradzaman, M.; Martínez, C. S.; Mul, G. Effect of partial pressure on product selectivity in Cu-catalyzed electrochemical reduction of CO₂. *Sustainable Energy & Fuels* **2020**, *4* (10), 5195–5202.

(59) Huber, B.; Roling, B. Development of a Ag/Ag⁺ micro-reference electrode for electrochemical measurements in ionic liquids. *Electrochim. Acta* **2011**, *56* (19), 6569–6572.

(60) Shen, X.; Sinclair, N.; Wainright, J.; Akolkar, R.; Savinell, R. Evaluating and developing a reliable reference electrode for choline chloride based deep eutectic solvents. *J. Electrochem. Soc.* **2020**, *167* (8), No. 086509.

(61) Izutsu, K. Reference electrodes for use in nonaqueous solutions. *Handb. Ref. Electrodes* **2013**, 145–187.

(62) Smith, T. J.; Stevenson, K. J., 4 - Reference Electrodes. In *Handbook of Electrochemistry*, Zoski, C. G., Ed. Elsevier: Amsterdam, 2007; pp 73–110.

(63) García Rey, N.; Dlott, D. D. Structural transition in an ionic liquid controls CO₂ electrochemical reduction. *J. Phys. Chem. C* **2015**, *119* (36), 20892–20899.

(64) Leung, K. Y.; McCrory, C. C. L. Effect and Prevention of Trace Ag⁺ Contamination from Ag/AgCl Reference Electrodes on CO₂ Reduction Product Distributions at Polycrystalline Copper Electrodes. *ACS Applied Energy Materials* **2019**, *2* (11), 8283–8293.

(65) Roger, I.; Symes, M. D. Silver Leakage from Ag/AgCl Reference Electrodes as a Potential Cause of Interference in the Electrocatalytic Hydrogen Evolution Reaction. *ACS Appl. Mater. Interfaces* **2017**, *9* (1), 472–478.